
Symplectic Gaussian Process Dynamics

Katharina Ensinger
Bosch Center for
Artificial Intelligence,
Renningen, Germany

katharina.ensinger@bosch.com

Friedrich Solowjow
Max Planck Institute
for Intelligent Systems,
Stuttgart, Germany

Michael Tiemann
Bosch Center for
Artificial Intelligence,
Renningen, Germany

Sebastian Trimpe
Institute for Data Science
in Mechanical Engineering,
RWTH Aachen University,
Aachen, Germany

Abstract

Dynamics model learning is challenging and at the same time an active field of research. Due to potential safety critical downstream applications, such as control tasks, there is a need for theoretical guarantees. While GPs induce rich theoretical guarantees as function approximators in space, they do not explicitly cope with the time aspect of dynamical systems. However, propagating system properties through time is exactly what classical numerical integrators were designed for. We introduce a recurrent sparse Gaussian process based variational inference scheme that is able to discretize the underlying system with any explicit or implicit single or multistep integrator, thus leveraging properties of numerical integrators. In particular we discuss Hamiltonian problems coupled with symplectic integrators producing volume preserving predictions.

1 Introduction

Many real-world systems can be described by an autonomous continuous time dynamical system. In practice, it is impossible to observe continuous state trajectories since noisy observations are, for example, given by sensor data. Therefore the dynamics model has to be discretized. Numerical integrators, which are applied to simulation tasks, provide different discretization strategies with specific properties and guarantees as higher-order approximation or preservation of the energy. To address the evolution over time, the system is typically discretized with one step ahead predictions, which can be identified with the explicit Euler method. To learn an unknown model from sensor data, Gaussian

processes are a powerful tool providing guarantees as a function approximator for the dynamics model function (Van Der Vaart and Van Zanten, 2011) and uncertainty estimation for the learned model (Vinogradska et al., 2016; Doerr et al., 2017). We propose a more flexible method for the discretization step in order to enforce structure for the Gaussian process model.

Consider a continuous time dynamics model

$$\dot{x}(t) = f(x(t)), \quad (1)$$

with $f : \mathbb{R}^d \rightarrow \mathbb{R}^d$ and f Lipschitz continuous, where x describes the state of the system. The model is learned from noisy observed data

$$\begin{aligned} x_1 + \psi_1, \dots, x_N + \psi_N &\in \mathbb{R}^d, \\ \psi_n &\sim \mathcal{N}(0, \text{diag}(\sigma_{n,1}^2, \dots, \sigma_{n,d}^2)), \end{aligned}$$

with $x_n = x(t_n)$. Due to the discrete nature of the data samples, the most intuitive approach is to model the one step ahead predictions

$$x_{n+1} = g(x_n), \quad (2)$$

where g is a Gaussian process, which is the predominant approach for GP dynamics model learning (Deisenroth and Rasmussen, 2011; Frigola et al., 2014; Doerr et al., 2018; Buisson-Fenet et al., 2020). The key observation for our method is that this discretization can be identified with the explicit Euler method

$$x_{n+1} = x_n + hf(x_n). \quad (3)$$

by identifying $g(x_n)$ with $x_n + hf(x_n)$, which is common for training Gaussian process dynamics as well.

From numerical analysis, disadvantages are known for the explicit Euler method. It is suboptimal in terms of accuracy and leads to unstable predicted trajectories for stiff differential equations. Furthermore it is unrealistic for physical systems since no energy preservation is included. In contrast, symplectic integrators preserve the energy of Hamiltonian systems and thus keep this

important property of the underlying system. This provides stable long-term behaviour. Thus, we propose to leverage the structure and additional benefits from more complex numerical integrator schemes, such as implicit and/or symplectic integrators. This entails replacing the one step integrator (2) or (3) with a more powerful numerical integrator, which is the key idea of this paper. In this work, we will consider general linear numerical integrators (Hairer et al., 1987) which can be written

$$\begin{aligned} x_{n,i} &= h \sum_{j=1}^s a_{ij} f(x_{n,j}) + \sum_{j=0}^k u_{ij} x_{n-j}, \quad i = 1, \dots, s \\ x_{n+1} &= h \sum_{j=1}^s b_j f(x_{n,j}) + \sum_{j=0}^k v_j x_{n-j}, \end{aligned} \quad (4)$$

where $x_{n,i}$ are the internal stages at time n , $s \in \mathbb{N}_0$ and x_{n-j} are $k \in \mathbb{N}_0$ previously calculated points. The parameters $a_{ij}, b_j, u_{ij}, v_j \in \mathbb{R}$ determine the properties of the method, e.g., the stability radius of the method (Hairer and Wanner, 1996) or whether it is symplectic (Hairer et al., 2006). If $a_{ij} > 0$ for $j \geq i$, Eq. (4) requires the numerical solution of a nonlinear system of equations (Deuffhard, 2011). For the better clarity of the proposed method the numerical integrator (4) is written

$$x_{n+1} = x_n + h\phi(x_{n+1}, x_n, \dots, x_{n-k}) \quad (5)$$

When simulating a system f , any discretization scheme will introduce a biased discretization error. In theory, the learned dynamics model can compensate for the discretization error which would suggest that every discretization choice could be made to perform equally well. This also implies that it is possible to train stable and symplectic systems with a simple explicit discretization. However, due to the observation noise and the training error, or if predictions are required in the extrapolation regime during simulation, properties such as Hamiltonian or volume preservation are no longer guaranteed. If, on the other hand, a discretization scheme is applied which is symplectic or has a large stability radius, it should be easier to achieve these properties during prediction, which has also been observed empirically (Haber and Ruthotto, 2017; Queiruga et al., 2020). This is particularly desirable if a system is known or assumed to be asymptotically stable or Hamiltonian, in which case the *learned Hamiltonian* is guaranteed to be preserved when a symplectic discretization scheme is applied. While it is possible to learn the model from a continuous point-of-view, treating the vector field f —and not the discretization ϕ —as the sole object of interest (Heinonen and d’Alché Buc, 2014; Greydanus et al., 2019), it remains an open question how to automatically choose

the most appropriate discretization for the learned model. Our Gaussian process model is trained with variational inference based on a sparse Gaussian process approach that provides the necessary flexibility. These approach is common in state-space model literature (Doerr et al., 2018), since exact inference is intractable when multiple evaluations of the GP at unknown states is required. Here, a method is introduced that discretizes the dynamic system with any numerical integration method, including implicit methods, symplectic methods, higher order methods and multistep methods in order to benefit from the specific properties. We will focus here on symplectic methods for Hamiltonian systems. A GP model is constructed that is volume preserving by design, approximating the Hamiltonian directly for which a symplectic integrator keeps this quantity. This leads to stable training and predictions. For separable Hamiltonians an explicit scheme is introduced. For general non separable Hamiltonians, an implicit symplectic integrator is required for which the reparameterization trick (Kingma and Welling, 2013) is derived in a declarative model setting (Gould et al., 2019). To our knowledge, there exists no learning methods that exploit volume preserving trajectories for training and predictions based for non separable Hamiltonians.

In summary, the main contributions of this paper are

- A general and flexible probabilistic learning framework that is applicable to each numerical integrator leveraging specific properties;
- A variational inference based approach to train implicit transitions for Gaussian process-based models;
- An application to separable and non separable Hamiltonian systems providing volume preserving predictions, thus providing long-term stability.

2 Related work

The related literature is split into the following aspects: dynamic model learning, implicitly defined learning problems and leveraging Hamiltonian structure.

Dynamic model learning methods can be addressed by a continuous or a discrete time model. The field of dynamic model learning has been surveyed in Nguyen-Tuong and Peters (2011). Gaussian process gradient matching methods can be applied to estimate the parameters of a parametrized continuous time dynamic model, where the discrepancy between the time derivative of Gaussian process interpolants and the parametrized ordinary differential equation are minimized (Wenk et al., 2019). Thus, general knowledge of

the structure is required. An adaptive gradient matching algorithm by sampling from the joint distribution of the ODE parameters and GP hyperparameters was introduced (Dondelinger et al., 2013). There exist few methods for learning continuous time dynamics from completely unknown models. The gradient matching approach is extended to nonparametric ODEs in Heinonen and d’Alché Buc (2014) in order to address this problem. The problem can also be approached by modeling the ODE with a sparse input Gaussian process leading to an additional ODE system that can be solved up to the accuracy of an arbitrary numerical ODE solver in order to learn the unknown parameters (Heinonen et al., 2018).

A common approach for learning discrete time models are Gaussian process state-space models (Turner et al., 2010; Wang et al., 2008; Lindholm et al., 2015). With the tools of state-space models, also discrete dynamic models can be learned. A variational inference model based on sparse Gaussian Processes was introduced in Frigola et al. (2014). Previous state-space models were improved by introducing a recurrent scheme that maintains the true latent state distribution (Doerr et al., 2018). This enables robustness and scalability. Recently an extension to such recurrent methods was proposed that samples from the true posterior distribution (Ialongo et al., 2019). Our proposed method is based on the state-space idea learning discrete time dynamics as well. But in contrast to state-space model literature the discretization step is more flexible and is chosen according to desired properties.

Training with implicit transitions has been done for neural networks. There exists literature that introduces implicit problems as layers (Gould et al., 2019). The implicit function theorem is employed to backpropagate through the layers. A neural network with infinitely many layers was trained by implicitly defining the equilibrium of the network (Bai et al., 2019). Implicit transitions have not been applied to Gaussian processes yet, which we propose.

Including Hamiltonian structure into learning, in order to keep physical properties of the system, is an important problem addressed by many sides. Neural networks were used to leverage Hamiltonian structure. Since they are powerful in terms of performance we do an experimental comparison against them. Neural networks are able to learn a separable Hamiltonian from data (Greydanus et al., 2019). The Hamiltonian neural network approach was extended by a recurrent neural network coupled with a symplectic integrator in Chen et al. (2019). In Zhong et al. (2020), a neural network was trained to learn a Hamiltonian system with control. The stable property of symplectic integrators is leveraged to build the architecture of a neural network by

introducing symplectic transitions between the layers of a neural network (Haber and Ruthotto, 2017).

3 Technical background

In this section, we give an overview of well known technical results that we need. Later, in Section 4, we introduce new concepts.

3.1 Variational sparse Gaussian process

A Gaussian process (Rasmussen and Williams, 2005) can be interpreted as a distribution over functions $f : \mathbb{R}^d \rightarrow \mathbb{R}$. Similar to a normal distribution a GP is fully determined by its mean $m(x)$ and covariance function $k_{x,y}$. We assume the prior mean to be zero. For direct training, the GP predictive distribution is obtained by conditioning on observed data X, y . To be able to deal with large datasets, the Gaussian process can be sparsified by introducing pseudo inputs (Titsias, 2009) since vanilla GP regression has a computational complexity of $\mathcal{O}(n^3)$ (Liu et al., 2018). Here, pseudo inputs $\xi = [\xi_1, \dots, \xi_P]$ and targets $z = [z_1, \dots, z_P]$ are introduced as proposed in (Hensman et al., 2013) and applied in (Doerr et al., 2018). The predictive distribution f^* at an input x^* is conditioned on the inducing points

$$\begin{aligned} p(f^* | x^*, f, X) &\approx p(f^* | x^*, \xi), \\ p(z) &= \mathcal{N}(0, k_{\xi, \xi}). \end{aligned} \quad (6)$$

Next, consider a variational distribution at the sparse inputs. The variational approximation for the inducing points is given

$$q(z) = \mathcal{N}(\mu, \Sigma), \quad (7)$$

where μ and Σ are adapted during training. The Gaussian process is again conditioned on the inducing points and the inducing outputs are marginalized out. At an input x^* , it holds

$$f(x^*) \sim \mathcal{N}(\mu(x^*), \sigma^2(x^*)),$$

with

$$\begin{aligned} \mu(x^*) &= \alpha(x^*)^T \mu \\ \sigma^2(x^*) &= k_{x^*, x^*} - \alpha(x^*)^T (k_{\xi, \xi} - \Sigma) \alpha(x^*) \end{aligned} \quad (8)$$

and $\alpha(x^*) = k_{x^*, \xi} k_{\xi, \xi}^{-1}$. For the derivative $\frac{\partial f}{\partial x^*}$ it holds that

$$\frac{\partial f}{\partial x^*} \sim \mathcal{N}(\mu'(x^*), K'(x^*)),$$

with

$$\begin{aligned} \mu'(x^*) &= \left(\frac{d\alpha(x^*)}{dx^*} \right)^T \mu \\ K'(x^*) &= \frac{\partial k_{x^*, x^*}}{\partial x^* \partial x^*} - \left(\frac{d\alpha(x^*)}{dx^*} \right)^T (k_{\xi, \xi} - \Sigma) \left(\frac{d\alpha(x^*)}{dx^*} \right). \end{aligned} \quad (9)$$

A detailed derivation of the sparse Gaussian process with derivative observations was made in Yang et al. (2018).

3.2 Variational inference scheme

The numerical integrator requires multiple evaluations of the nonlinear GP dynamics model f . Thus, the target value is no longer normal distributed, making direct inference intractable. We therefore approximate the model with variational inference. Similar variational inference schemes have been applied in Föll et al. (2019); Frigola et al. (2014). We follow the approach applied in Doerr et al. (2018). Consider noisy observed data

$$\begin{aligned}\hat{x}_n &= x_n + \psi_n, \\ \psi_n &\sim \mathcal{N}(0, \text{diag}(\sigma_{n,1}^2, \dots, \sigma_{n,d}^2)).\end{aligned}\quad (10)$$

The probability $p(x_n)$ for the observed data is factorized and approximated by a variational distribution. The scheme is based on pseudo inputs (6)-(9) and the probability

$$p(x_{n+1}|x_n, z), \quad (11)$$

for the noise free data, which is determined by the numerical discretization (5). Inducing the numerical scheme and calculating the gradients is presented in Section 4. Factorizing the joint distribution of observations, noise-free states and inducing inputs yields

$$\begin{aligned}p(\hat{x}_{1:N}, x_{0:N}, z) \\ = \prod_{n=0}^{N-1} p(\hat{x}_{n+1}|x_{n+1})p(x_{n+1}|x_n, z)p(z)p(x_0).\end{aligned}\quad (12)$$

The variational distribution q is chosen

$$q(x_{0:N}, z) = \prod_{n=0}^{N-1} p(x_{n+1}|x_n, z)q(z)p(x_0), \quad (13)$$

with the variational distribution $q(z)$ of the inducing inputs and targets from Section 3.1. The model is adapted by maximizing the Evidence Lower Bound (ELBO)

$$\begin{aligned}\log p(\hat{x}_{1:N}) &\geq \mathbb{E}_{q(x_{0:N}, z)} \left[\log \frac{p(\hat{x}_{1:N}, x_{0:N}, z)}{q(x_{0:N}, z)} \right] \\ &= \sum_{n=1}^N \mathbb{E}_{q(x_{0:N}, z)} [\log p(\hat{x}_n|x_n)] \\ &\quad - KL(p(z)||q(z)) \\ &=: \mathcal{L}.\end{aligned}\quad (14)$$

The ELBO \mathcal{L} is maximized by a sampling based stochastic gradient method. Samples from the variational distribution $q(\hat{x}_{0:N}, z)$ are drawn and the hyperparameters are adapted. The reparametrization procedure and the calculation of the gradients is described in Section 4.

3.3 Predictions

During training the parameters of $q(z)$ are adapted. Sampling a trajectory (x_1, \dots, x_N) with initial value x_0 can be done by gradually sampling from $p(x_{n+1}|x_n, z)q(z)$, $n = 1, \dots, N-1$. An approximation that omits sampling is provided by propagating the mean, which is not as exact.

4 Embedding arbitrary numerical integrators into the GP model

After establishing the basics in GP regression and variational inference, we will address how to embed numerical integrators into the presented framework. Further, we show how to backpropagate through the method.

4.1 Main idea

In order to train the GP dynamics model on an arbitrary numerical discretization, we need to apply the method to the GP dynamics model. The variational inference scheme coupled with the sparse GP we introduced in Section 3 provides the necessary flexibility and bridges to the original idea. Due to the general approach we are now able to evaluate the GP at arbitrary points. The transition probability $p(\hat{x}_{n+1}|\hat{x}_n, z)$ in (12) and (13) is determined by the numerical integrator. We solve the problem of embedding the integrator with a sampling based approach and apply the reparametrization trick. Thus, we draw a realization of the numerical integrator from the current model in each training step by sampling from a normal distribution. Mean and variance are determined by the sparse GP and described in Section 3.1. We extend the approach to implicit problems leading to a nonlinear system of equations that has to be solved in order to evaluate a sample. The following section describes the technical details of the sampling based method. The parameters are adapted with stochastic gradient descent.

4.2 Reparametrization

Consider the transition probability $p(x_{n+1}|x_n, z)$ in (12) and (13) that is determined by the numerical integrator

$$x_{n+1} = x_n + h\phi(x_{n+1}, x_n, \dots, x_{n-k}). \quad (15)$$

Calculating $\phi(x_{n+1}, x_n, \dots, x_{n-k})$ in (15) requires the evaluation of the dynamic function f at several inputs. The evaluations of $f(u)$ at points u that contribute to $\phi(x_n)$ are assumed to be normal distributed for all u with expectation $\mu(u)$ and covariance matrix $\Sigma(u)$. Usually each output dimension $i = 1, \dots, d$

of $p(f_i(u)|u, z)$ is modeled separately by d independent sparse Gaussian processes (6)-(8) and a set of sparse inputs ξ_i and targets z_i with $\xi = \xi_1, \dots, \xi_d$ and $z = z_1, \dots, z_d$ is introduced for each dimension, leading to

$$\begin{aligned} \mu(u) &= (\mu_1(u), \dots, \mu_d(u)) \\ \Sigma(u) &= \text{diag}(\sigma_1^2(u), \dots, \sigma_d^2(u)). \end{aligned} \quad (16)$$

But also a derivative Gaussian process (9) or a multi-output GP (Álvarez et al., 2010) can be considered to model f .

The ELBO (14) is approximated and minimized by a sampling based approach coupled with stochastic gradient descent in order to optimize the hyperparameters. This requires drawing samples from the variational distribution $q(x_{0:N}, z)$. To be able to calculate gradients with respect to the hyperparameters the reparametrization trick (Kingma and Welling, 2013) is applied. To gain the initial value x_0 the reparametrization trick is applied by sampling from $\mathcal{N}(\hat{x}_0, \text{diag}(\sigma_{n,1}^2, \dots, \sigma_{n,d}^2))$,

$$x_0 = \hat{x}_0 + \epsilon \sqrt{\text{diag}(\sigma_{n,1}^2, \dots, \sigma_{n,d}^2)}, \quad (17)$$

with $\epsilon \sim \mathcal{N}(0, 1)$.

To sample x_{n+1} from $p(x_{n+1}|x_n, z)$ the reparametrization trick is applied again. The method can be applied to each conventional explicit or implicit single or multi-step method. The evaluations of the dynamic function f at several inputs is done by drawing from

$$f(u) \sim \mathcal{N}(\mu(u), \Sigma(u)).$$

Let the Cholesky decomposition of the covariance matrix be $\Sigma(u) = L(u)L(u)^T$. A calculation of $f(u)$ is done by

$$f(u) = \mu(u) + L(u)\epsilon. \quad (18)$$

In the next step, the reparametrization step is illustrated by applying to a higher order explicit method and a simple implicit method. All methods are operating on independent sparse Gaussian processes for each dimension. Non separable Hamiltonian problems in Section 5.1 provide an application to the derivative sparse GP (9).

For illustration consider the explicit midpoint method as an example for a higher order Runge-Kutta method

$$x_{n+1} = x_n + hf \left(x_n + \frac{h}{2} f(x_n) \right). \quad (19)$$

Applying the reparametrization trick yields

$$\begin{aligned} v &= x_n + \frac{h}{2} (\mu(x_n) + L(x_n)\epsilon) \\ x_{n+1} &= x_n + h(\mu(v) + L(v)\epsilon). \end{aligned} \quad (20)$$

For implicit solvers the reparametrization yields a system of equations that has to be solved in order to evaluate at the next time step. Consider the implicit Euler method as the simplest implicit method

$$x_{n+1} = x_n + hf(x_{n+1}). \quad (21)$$

Applying the reparametrization trick yields

$$x_{n+1} = x_n + h(\mu(x_{n+1}) + L(x_{n+1})\epsilon). \quad (22)$$

Thus, x_{n+1} solves the minimization problem

$$\begin{aligned} x_{n+1} &= \arg \min_v g(x_n, v) \\ &= \arg \min_v \|v - x_n - h(\mu(v) + \epsilon L(v))\|^2. \end{aligned} \quad (23)$$

4.3 Gradients

The ELBO (14) is minimized by applying stochastic gradient descent to the hyperparameters. The hyperparameters contain the parameters that adapt $q(z)$ depending on the chosen variational distribution. When conditioning on the sparse Gaussian process (6)-(8) the hyperparameters include $(\mu_{1:d}, \sigma_{f,1:d}, \theta_{1:d}^{GP}, \sigma_{n,1:d})$ with Gaussian hyperparameters $\theta_{1:d}^{GP}$. For the ARD kernel (Rasmussen and Williams, 2005)

$$k(x, x') = \sigma_f^2 \exp\left(-\frac{\|x - x'\|^2}{2l^2}\right) \quad (24)$$

and d independent GPs it holds that

$$\theta^{GP} = (\sigma_{f,1:d}, l_{1:d}). \quad (25)$$

To compute the gradients, it is necessary to compute

$$\frac{dx_{n+1}}{d\theta}. \quad (26)$$

For an explicit scheme $x_{n+1} = x_n + h\phi(u)$ with $u = (x_n, \dots, x_{n-k})$, the gradient computation is straightforward

$$\begin{aligned} \frac{dx_{n+1}}{d\theta} &= \frac{dx_n}{d\theta} + h \left(\frac{d\phi(u)}{d\theta} \right) \\ &= \frac{dx_n}{d\theta} + \left(\frac{\partial \phi(u)}{\partial \theta} \right) \left(\frac{du}{d\theta} \right). \end{aligned} \quad (27)$$

The gradient is backpropagated through time by the dependence on $\left(\frac{du}{d\theta}\right)$ and $\left(\frac{dx_n}{d\theta}\right)$.

For the implicit solvers a nonlinear equation has to be solved. It holds that

$$x_{n+1} = \arg \min_v g(u, v), \text{ with } u = (x_n, \dots, x_{n-k}), \quad (28)$$

for some function $g(u, v)$. The corresponding minimization problem for the implicit Euler function is presented

in (23). As pointed out in Gould et al. (2019), the implicit function theorem can be applied in order to calculate the gradients of the implicit transition function. It holds that

$$\begin{aligned} \frac{dx_{n+1}}{d\theta} &= \frac{dx_{n+1}}{du} \frac{du}{d\theta} \\ &= -\left(g_{uu}^2(u, x_{n+1})\right)^{-1} g_{uv}^2(u, x_{n+1}) \left(\frac{du}{d\theta}\right). \end{aligned} \quad (29)$$

By the dependence on $\left(\frac{du}{d\theta}\right)$ the gradient is backpropagated through time again.

4.4 Propagating the uncertainty

For the explicit Euler method, there exist techniques to propagate the uncertainty. This section shall illustrate that these techniques can be extended to other numerical methods by illustrating the approach for the implicit Euler scheme. Thus, the proposed method is not a limitation. For the ARD kernel the uncertainty of a trajectory can be propagated via exact moment matching as previously applied in Deisenroth and Rasmussen (2011). The algorithm can be extended to sparse GPs by applying the calculation rules for noisy input Gaussian processes (Bijl et al., 2017). The probability of the states $p(x_n)$ is approximated by a Gaussian distribution

$$x_n \sim \mathcal{N}(\mu_n, \sigma_n), \quad (30)$$

with $\sigma_n = \text{diag}(\sigma_{n,1}, \dots, \sigma_{n,d})$.

For explicit numerical schemes, previous work can easily be extended. For implicit schemes, this is not as straightforward, but a normal distribution can be propagated as well by solving a system of equations. The derivation is moved to the appendix.

5 Applications

With the method proposed in Section 4, any numerical integration scheme can be embedded and used for GP dynamics learning. In this section, we present the application of the embedding scheme in Section 4 to Hamiltonian problems coupled with symplectic integrators. Many physical models can be modeled with Hamiltonians (Salmon, 2003; Sakurai, 1994; Girvin and Yang, 1994). Symplectic integrators are volume preserving for Hamiltonian systems. Since Hamiltonians keep a property similar to the total energy, a system discretized with a symplectic integrator keeps it as well. For separable Hamiltonians these integrators are explicit methods for general Hamiltonians they are implicit. By modeling the Hamiltonian itself and training and predicting with a symplectic integrator the learned Hamiltonian is kept constant among the trajectory inducing stability to training and predictions.

5.1 Hamiltonian systems

A broad class of physical system can be written as Hamiltonian system $x(t) = (p(t), q(t))^T$ with

$$\begin{aligned} \dot{p}(t) &= -H_q(p, q) \\ \dot{q}(t) &= H_p(p, q) \end{aligned} \quad (31)$$

and

$$p, q \in \mathbb{R}^d. \quad (32)$$

The Hamiltonian H is similar to the total energy and constant among a trajectory.

5.1.1 Separable Hamiltonian

An important class of Hamiltonian problems are separable Hamiltonians. A broad class of real world systems can be modeled by separable Hamiltonians,

$$H(p, q) = T(p) + V(q). \quad (33)$$

Then for the dynamic system it holds that

$$\begin{aligned} \dot{p}(t) &= -V'(q) \\ \dot{q}(t) &= T'(p) \end{aligned} \quad (34)$$

for some $V : \mathbb{R}^d \rightarrow \mathbb{R}^d$ and $T : \mathbb{R}^d \rightarrow \mathbb{R}^d$. By training independent sparse GPs on $V'_1(q), \dots, V'_d(q)$ and $T'_1(p), \dots, T'_d(p)$ and applying a symplectic integrator, the predictions are volume preserving by design. By training derivative sparse GPs on $V'_1(q), \dots, V'_d(q)$ and $T'_d(p), \dots, T'_d(p)$ an additional approximation to the Hamiltonian is applied via the GPs for $V_1(q), \dots, V_d(q)$ and $T_1(p), \dots, T_d(p)$. The evolving hyperparameters are $(\theta_{1:d}^{GP,p}, \theta_{1:d}^{GP,q}, \mu_{1:d}^p, \mu_{1:d}^q, \Sigma_{1:d}^p, \Sigma_{1:d}^q, \sigma_{n,1:d})$. Consider for example the symplectic Euler method

$$\begin{aligned} p_{n+1} &= p_n - hV'(q_n) \\ q_{n+1} &= q_n + hT'(p_{n+1}). \end{aligned} \quad (35)$$

Then (35) is reparametrized as described in Section 4.2 by sampling from V' and T' and the scheme can be embedded into the variational inference scheme.

5.1.2 Non separable Hamiltonian

The general Hamiltonian system (31) is an application to implicit methods since symplectic integrators are implicit in general. An example for a symplectic integrator is the implicit midpoint rule

$$x_{n+1} = x_n + hJ^{-1}\nabla H\left(\frac{x_n + x_{n+1}}{2}\right), \quad (36)$$

with

$$J^{-1} = \begin{pmatrix} 0 & -1 \\ 1 & 0 \end{pmatrix}. \quad (37)$$

To guarantee area preserving predictions it has to be assured that the learned system itself is a Hamiltonian system and that samples are drawn from a Hamiltonian. The Hamiltonian is assumed to be modeled by a sparse GP (eqref:sgpd-8). Sampling from (36) requires evaluating the gradient ∇H . For the gradient ∇H it holds that

$$\nabla H(u) \sim \mathcal{N}(\mu'(u), K'(u)) \quad (38)$$

with $\mu'(u)$ and $K'(u)$ defined in (9). In addition to preserving the volume and total energy we achieved that the outputs are correlated. The usual modeling assumption of independent GPs is a simplification of the underlying system. This problem could also be addressed with multi-output GPs (Álvarez et al., 2010), but here we derived the correlation naturally from the underlying physical law and kept its properties.

6 Experiments

The symplectic Gaussian process dynamic model (SGPD) is compared to the explicit Euler method, which corresponds to the standard state-space approach as explained in Section 1 and to the Hamiltonian neural network (Greydanus et al., 2019) with their code. The main libraries used for computation are Paszke et al. (2019) and Harris et al. (2020). For the plots and presentation Hunter (2007) was used.

6.1 Separable Hamiltonian

We took two examples that were also considered in Greydanus et al. (2019). We train our Gaussian process with the approach in Section 5.1.1 by modeling the Hamiltonian $T(p)+V(q)$ itself with independent GPs on T and V and its derivatives \dot{p} and \dot{q} with the derivatives of the GPs. This provides specific information for the physical system. By including this prior knowledge we especially expect an advantage compared to the standard explicit Euler approach. Training data are generated from ground truth and noise with variance $\sigma^2 = 0.1$ is added. We choose the same initialization of hyperparameters and number of inducing points for the explicit Euler scheme and our SGPD method. The inducing points are initialized uniformly distributed between the minimum and maximum of the observed data. The trajectory is split in subtrajectories of length 10 for training our SGPD model and the explicit Euler model. We compare the L^2 -error of the error curves between approximation and ground truth. Table 1 shows the results for the two separable systems.

Ideal mass spring Consider the ideal mass spring system

$$H(p, q) = 0.5p^2 + 0.5q^2 \quad (39)$$

with $p, q \in \mathbb{R}$. The predictions of the mass spring states p are shown in Figure 1a in contrast to ground truth and noisy observations. The evolution of L^2 -error among the rollout is illustrated in Figure 2a for the three methods. We observed that for the same configuration of inducing inputs and hyperparameters the explicit Euler method needs more training steps to converge compared to our SGPD approach.

Ideal pendulum Consider an ideal pendulum

$$H(p, q) = (1 - 6 \cos(p)) + \frac{p^2}{2}. \quad (40)$$

The predictions of the pendulum states p are illustrated in Figure 1b in contrast to ground truth and noisy observations. The evolution of the L^2 -error along the trajectory is shown in Figure 2b. We observed that our SGPD approach works for longer trajectories as well, while the explicit Euler method fails. Details of this additional experiment are moved to the appendix.

Table 1: L^2 -error for separable Hamiltonian

system	SGPD	Euler	HNN
mass spring	0.1951	0.8327	0.256
pendulum	0.73	4.69	2.69

The results for both experiments suggest that the symplectic method adapts faster and more stable to Hamiltonian systems with a smaller amount of inducing points than the standard explicit Euler approach. This observation coincides with the results from Haber and Ruthotto (2017), where a ResNet was trained with symplectic transitions between the layers, stabilizing training. Our explicit SGPD method provides the smallest L^2 -error between approximation and ground truth compared to the other methods.

Furthermore we provide theoretical guarantees as described in Section 5 and train a probabilistic method in contrast to the deterministic Hamiltonian neural network. Note that the Hamiltonian neural network computes predictions by solving an initial values problem with a small tolerance. This leads to multiple internal time steps per sampling frequency. The SGPD method commits to a fixed time step size and thus compensates the numerical error for fixed time step predictions already during training. However, by integrating additional internal steps per sampling frequency during training a continuous time dynamic model could be learned up to an arbitrary accuracy.

6.2 Non separable Hamiltonian

We compare in terms of L^2 -error and energy in order to show that the energy is not preserved by approximating

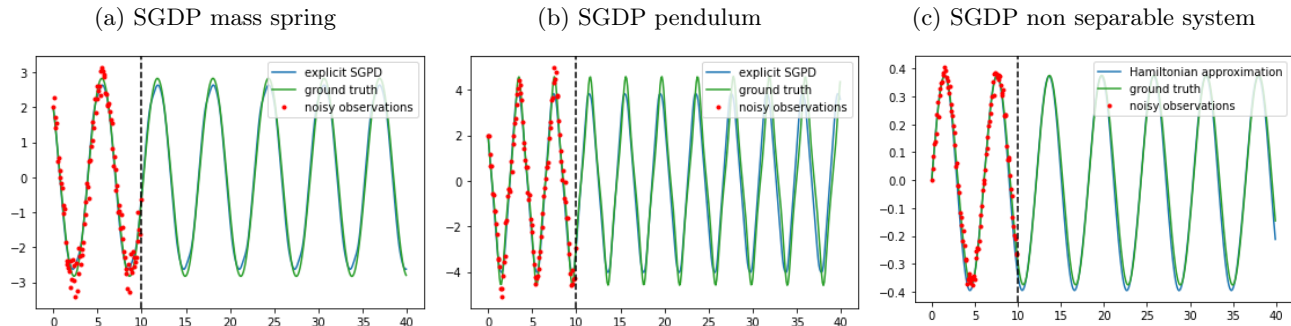


Figure 1: Results for the experiments. Shown are trajectories over time with SGPD (blue) for the separable Hamiltonians 1a 1b and the non separable Hamiltonian 1c compared with ground truth (green). The training horizon is marked with red dots

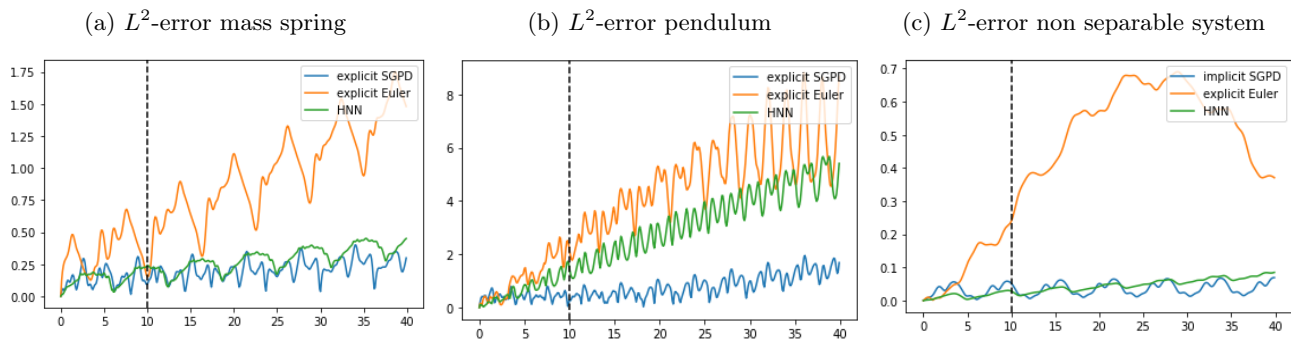


Figure 2: Corresponding L^2 -errors of the rollouts (2a–2c). L^2 -errors of our SGPD model (blue), the standard explicit Euler method (green) and the Hamiltonian Neural Network model from Greydanus et al. (2019).

with the HNN approach and the standard explicit Euler approach. We train on subtrajectories of length 10 and use the same amount of inducing points for the implicit SGPD and the explicit Euler method.

Non separable system Consider the Hamiltonian

$$H(p, q) = \frac{1}{2} [(q^2 + 1)(p^2 + 1)]. \quad (41)$$

The approach in Section 5.1.2 is made by applying the implicit midpoint rule (36). As step size for training and predictions $h = 0.1$ is chosen. Training data are generated from ground truth and noise with variance $\sigma^2 = 0.0005$ is added.

Table 2: Non separable Hamiltonian

quantity	SGPD	Euler	HNN
L^2	0.03	0.42	0.04
energy mean	0.570	0.574	0.554
energy std deviation	0.003	0.002	0.002

The evolution of the state p in contrast to ground truth and noisy observations is illustrated in Figure 1c. The evolution of the L^2 -error over time is shown in 2c for

all three methods. The training horizon is marked. We further compare the three methods in terms of L^2 -error and energy. The L^2 error of the error curve between approximation and ground truth is considered for the predictions. For the total energy the mean and the standard deviation among the trajectory are computed. The results are shown in Table 2. Especially in terms of energy preservation our implicit SGPD is the most stable. The mean of the energy around the trajectory is closest to the ground truth energy 0.57 and the energy fluctuates least. Note that energy preservation does not correspond to L^2 -error preservation.

7 Conclusion and future work

We introduce a recurrent sparse GP based variational inference scheme that is able to discretize the underlying system with any explicit or implicit single or multistep integrator. We focus on Hamiltonian systems coupled with symplectic integrators, thus enforcing energy preservation to the predictions for separable and non separable Hamiltonian systems. Training was stabilized by the volume preserving quantity of symplectic integrators. Due to its architecture, the algorithm could be extended easily to a wider class of problems, such as

state-space models. This enables learning Hamiltonians with only partially observed states as well. Another possibility is leveraging the scheme to learn continuous time dynamics by scaling down the step size.

7.0.1 Acknowledgements

We thank Barbara Rakitsch and Alexander von Rohr for helpful discussions.

Bibliography

- Bai, S., Kolter, J. Z., and Koltun, V. (2019). Deep equilibrium models. In *Advances in Neural Information Processing Systems 32*, pages 690–701.
- Bijl, H., Schön, T., Wingerden, J. W., and Verhaegen, M. (2017). System identification through online sparse gaussian process regression with input noise. *IFAC Journal of Systems and Control*, 2:1–11.
- Buisson-Fenet, M., Solowjow, F., and Trimpe, S. (2020). Actively learning gaussian process dynamics. volume 120 of *Proceedings of Machine Learning Research*, pages 5–15. PMLR.
- Chen, Z., Zhang, J., Arjovsky, M., and Bottou, L. (2019). Symplectic recurrent neural networks. *arXiv:1909.13334*.
- Deisenroth, M. P. and Rasmussen, C. E. (2011). Pilco: A model-based and data-efficient approach to policy search. In *In Proceedings of the International Conference on Machine Learning*.
- Deuffhard, P. (2011). *Newton methods for nonlinear problems: affine invariance and adaptive algorithms*. Springer.
- Doerr, A., Daniel, C., Nguyen-Tuong, D., Marco, A., Schaal, S., Toussaint, M., and Trimpe, S. (2017). Optimizing long-term predictions for model-based policy search. In *Proceedings of 1st Annual Conference on Robot Learning (CoRL)*, volume 78, pages 227–238.
- Doerr, A., Daniel, C., Schiegg, M., Nguyen-Tuong, D., Schaal, S., Toussaint, M., and Trimpe, S. (2018). Probabilistic recurrent state-space models. In *Proceedings of the International Conference on Machine Learning (ICML)*.
- Dondelinger, F., Rogers, S., and Husmeier, D. (2013). Ode parameter inference using adaptive gradient matching with gaussian processes. In *Sixteenth International Conference on Artificial Intelligence and Statistics; AISTATS*.
- Föll, R., Haasdonk, B., Hanselmann, M., and Ulmer, H. (2019). Deep recurrent gaussian process with variational sparse spectrum approximation.
- Frigola, R., Chen, Y., and Rasmussen, C. (2014). Variational gaussian process state-space models. *Advances in Neural Information Processing Systems 27 (NIPS 2014)*, pages 3680–3688.
- Girvin, S. M. and Yang, K. (1994). *Modern condensed matter physics*. Cambridge University Press.
- Gould, S., Hartley, R., and Campbell, D. (2019). Deep declarative networks: A new hope. *arXiv:1909.04866*.
- Greydanus, S., Dzamba, M., and Yosinski, J. (2019). Hamiltonian neural networks. In *Advances in Neural Information Processing Systems 32*, pages 15379–15389.
- Haber, E. and Ruthotto, L. (2017). Stable architectures for deep neural networks. *Inverse Problems*, 34.
- Hairer, E., Lubich, C., and Wanner, G. (2006). *Geometric numerical integration: structure-preserving algorithms for ordinary differential equations*. Springer.
- Hairer, E., Nørsett, S., and Wanner, G. (1987). *Solving Ordinary Differential Equations I – Nonstiff Problems*. Springer.
- Hairer, E. and Wanner, G. (1996). *Solving Ordinary Differential Equations II – Stiff and Differential-Algebraic Problems*. Springer.
- Harris, C. R., Millman, K. J., van der Walt, S. J., Gommers, R., Virtanen, P., Cournapeau, D., Wieser, E., Taylor, J., Berg, S., Smith, N. J., Kern, R., Picus, M., Hoyer, S., van Kerkwijk, M. H., Brett, M., Haldane, A., del R’io, J. F., Wiebe, M., Peterson, P., G’erard-Marchant, P., Sheppard, K., Reddy, T., Weckesser, W., Abbasi, H., Gohlke, C., and Oliphant, T. E. (2020). Array programming with NumPy. *Nature*, 585(7825):357–362.
- Heinonen, M. and d’Alché Buc, F. (2014). Learning nonparametric differential equations with operator-valued kernels and gradient matching.
- Heinonen, M., Yildiz, C., Mannerström, H., Intosalmi, J., and Lähdesmäki, H. (2018). Learning unknown ODE models with gaussian processes. In *Proceedings of the 35th International Conference on Machine Learning*.
- Hensman, J., Fusi, N., and Lawrence, N. (2013). Gaussian processes for big data. *Uncertainty in Artificial Intelligence - Proceedings of the 29th Conference, UAI 2013*.
- Hunter, J. D. (2007). Matplotlib: A 2d graphics environment. *Computing in Science & Engineering*, 9(3):90–95.
- Ialongo, A. D., Van Der Wilk, M., Hensman, J., and Rasmussen, C. E. (2019). Overcoming mean-field approximations in recurrent Gaussian process models.

- In *Proceedings of the 36th International Conference on Machine Learning (ICML)*.
- Kingma, D. and Welling, M. (2013). Auto-encoding variational bayes. *ICLR*.
- Lindholm, A., Solin, A., Särkkä, S., and Schön, T. (2015). Computationally efficient bayesian learning of gaussian process state space models.
- Liu, H., Ong, Y., Shen, X., and Cai, J. (2018). When gaussian process meets big data: A review of scalable gps.
- Álvarez, M., Luengo, D., Titsias, M., and Lawrence, N. D. (2010). Efficient multioutput gaussian processes through variational inducing kernels. volume 9 of *Proceedings of Machine Learning Research*, pages 25–32. JMLR Workshop and Conference Proceedings.
- Nguyen-Tuong, D. and Peters, J. (2011). Model learning for robot control: A survey. *Cognitive processing*, 12:319–40.
- Paszke, A., Gross, S., Massa, F., Lerer, A., Bradbury, J., Chanan, G., Killeen, T., Lin, Z., Gimelshein, N., Antiga, L., Desmaison, A., Kopf, A., Yang, E., DeVito, Z., Raison, M., Tejani, A., Chilamkurthy, S., Steiner, B., Fang, L., Bai, J., and Chintala, S. (2019). Pytorch: An imperative style, high-performance deep learning library. In Wallach, H., Larochelle, H., Beygelzimer, A., Alché-Buc, F., Fox, E., and Garnett, R., editors, *Advances in Neural Information Processing Systems 32*, pages 8024–8035. Curran Associates, Inc.
- Queiruga, A. F., Erichson, N. B., Taylor, D., and Mahoney, M. W. (2020). Continuous-in-depth neural networks.
- Rasmussen, C. E. and Williams, C. K. I. (2005). *Gaussian Processes for Machine Learning (Adaptive Computation and Machine Learning)*. The MIT Press.
- Sakurai, J. J. (1994). *Modern quantum mechanics; rev. ed.* Addison-Wesley, Reading, MA.
- Salmon, R. (2003). Hamiltonian fluid mechanics. *Annual Review of Fluid Mechanics*, 20:225–256.
- Titsias, M. (2009). Variational learning of inducing variables in sparse gaussian processes. *Journal of Machine Learning Research - Proceedings Track*, pages 567–574.
- Turner, R., Deisenroth, M., and Rasmussen, C. (2010). State-space inference and learning with gaussian processes. *Journal of Machine Learning Research - Proceedings Track*, 9:868–875.
- Van Der Vaart, A. and Van Zanten, H. (2011). Information rates of nonparametric gaussian process methods. *Journal of Machine Learning Research*, 12(6).
- Vinogradska, J., Bischoff, B., Nguyen-Tuong, D., Romer, A., Schmidt, H., and Peters, J. (2016). Stability of controllers for gaussian process forward models. volume 48 of *Proceedings of Machine Learning Research*, pages 545–554, New York, New York, USA. PMLR.
- Wang, J., Fleet, D., and Hertzmann, A. (2008). Gaussian process dynamical models for human motion. *IEEE transactions on pattern analysis and machine intelligence*, 30:283–98.
- Wenk, P., Gotovos, A., Bauer, S., Gorbach, N., Krause, A., and Buhmann, J. M. (2019). Fast gaussian process based gradient matching for parameter identification in systems of nonlinear odes. In *Proceedings of the 22nd International Conference on Artificial Intelligence and Statistics (AISTATS)*, pages 1351–1360.
- Yang, A., Li, C., Rana, S., Gupta, S., and Venkatesh, S. (2018). *Sparse Approximation for Gaussian Process with Derivative Observations: 31st Australasian Joint Conference, Wellington, New Zealand, December 11-14, 2018, Proceedings*, pages 507–518.
- Zhong, Y. D., Dey, B., and Chakraborty, A. (2020). Symplectic ode-net: Learning hamiltonian dynamics with control.

Symplectic Gaussian Process Dynamics: Supplementary Materials

1 Propagating the uncertainty

Moment matching is often applied in order to propagate the uncertainty for the explicit Euler Gaussian process dynamic model (Deisenroth and Rasmussen, 2011)

$$x_{n+1} = x_n + hf(x_n). \quad (1)$$

The probability of the states $p(x_n)$ is approximated by a Gaussian distribution

$$x_n \sim \mathcal{N}(\mu_n, \Sigma_n). \quad (2)$$

For the ARD kernel (Rasmussen and Williams, 2005) exact moment matching can be applied to obtain $p(x_{n+1})$ from $p(x_n)$ and the Gaussian process mean and covariance. The example of the implicit Euler scheme illustrates that the approach can be extended to implicit integrators. Consider the implicit Euler scheme

$$x_{n+1} = x_n + hf(x_{n+1}), \quad (3)$$

with $f = (f_1, \dots, f_d)$ and independent sparse GPs $f_i(x)$. It holds that

$$f(x) \sim \mathcal{N}(\mu_f(x), \Sigma_f(x)), \quad (4)$$

with $\mu_f(x) = (\mu_f^1(x), \dots, \mu_f^d(x))$ and $\Sigma_f(x) = \text{diag}(\Sigma_f^1(x), \dots, \Sigma_f^d(x))$. Since the input x_{n+1} is assumed to be Gaussian distributed with mean μ_{n+1} and covariance matrix Σ_{n+1} a sparse GP with noisy inputs is obtained. It holds that

$$f(x_{n+1}) \sim \mathcal{N}(\hat{m}(\mu_{n+1}, \Sigma_{n+1}), \hat{\Sigma}(\mu_{n+1}, \Sigma_{n+1})), \quad (5)$$

where $\hat{m}(\mu_{n+1}, \Sigma_{n+1})$ and $\hat{\Sigma}(\mu_{n+1}, \Sigma_{n+1})$ can be obtained from formulae for noisy input sparse GPs.

For the predictive mean μ_{n+1} and the predictive covariance function Σ_{n+1} with (3) it holds that

$$\begin{aligned} \mu_{n+1} &= \mu_n + h\hat{m}(\mu_{n+1}, \Sigma_{n+1}) \\ \Sigma_{n+1} &= \Sigma_n + h^2\hat{\Sigma}(\mu_{n+1}, \Sigma_{n+1}) \end{aligned} \quad (6)$$

The system of equations (6) can be solved for μ_{n+1} and Σ_{n+1} . Let for each independent sparse GP f_i the kernel function be k^i with hyperparameters $(\sigma_{f,i}^2, L_i)$ and $L_i = \text{diag}(l_{i,1}^2, \dots, l_{i,d}^2)$. Let the set of sparse inputs be ξ . For clarity the set of sparse inputs is assumed to be equal for each dimension $i = 1, \dots, d$. Let the inducing outputs be z^i with $z^i \sim \mathcal{N}(\mu_\xi^i, \Sigma_\xi^i)$. The expressions for $\hat{m}_{n+1} = \hat{m}(\mu_{n+1}, \Sigma_{n+1})$ and $\hat{\Sigma}_{n+1} = \hat{\Sigma}(\mu_{n+1}, \Sigma_{n+1})$ can be obtained directly from Bijl et al. (2017)

$$\begin{aligned} \hat{m}_{n+1}^i &= (q^i)^T (k_{\xi,\xi}^i)^{-1} \mu_\xi^i, \\ \hat{\Sigma}_{n+1}^{i,i} &= \sigma_{f,i}^2 - \text{tr}((k_{\xi,\xi}^i)^{-1} (k_{\xi,\xi}^i - \Sigma_\xi^i) ((k_{\xi,\xi}^i)^{-1} Q^{i,i})) \\ &\quad + (\mu_\xi^i)^T (k_{\xi,\xi}^i)^{-1} Q^{i,i} (k_{\xi,\xi}^i)^{-1} \mu_\xi^i - [\hat{m}_{n+1}^i]^2 \\ \hat{\Sigma}_{n+1}^{i,j} &= (\mu_\xi^i)^T (k_{\xi,\xi}^i)^{-1} Q^{i,j} (k_{\xi,\xi}^j)^{-1} \mu_\xi^j - [\hat{m}_{n+1}^i \hat{m}_{n+1}^j]^2 \end{aligned} \quad (7)$$

with

$$\begin{aligned}
 q_l^i &= \frac{\sigma_{f,i}^2}{\sqrt{|\Sigma_{n+1}||\Sigma_{n+1}^{-1} + L_i^{-1}|}} \exp\left(-\frac{1}{2}(\xi_l - \mu_{n+1})^T (L_i + \Sigma_{n+1})^{-1} (\xi_l - \mu_{n+1})\right), \\
 Q_{kl}^{i,j} &= \frac{\sigma_{f,i}^2 \sigma_{f,j}^2}{\sqrt{|\Sigma_{n+1}||\Sigma_{n+1}^{-1} + L_i^{-1} + L_j^{-1}|}} \exp\left(-\frac{1}{2}(\xi_k - \xi_l)^T (L_i + L_j)^{-1} (\xi_k - \xi_l)\right), \\
 &\exp\left(-\frac{1}{2}(\tilde{x}_{kl}^{i,j} - \mu_{n+1})^T ((L_i^{-1} + L_j^{-1})^{-1} + \Sigma_{n+1})^{-1} (\tilde{x}_{kl}^{i,j} - \mu_{n+1})\right)
 \end{aligned} \tag{8}$$

and

$$\tilde{x}_{kl}^{i,j} = (L_i^{-1} + L_j^{-1})^{-1} (L_i^{-1} \xi_k + L_j^{-1} \xi_l). \tag{9}$$

2 Additional experiments

In the experimental section all experiments were trained with trajectories of length 10. We observed that the SGPD method can be trained with longer trajectories compared to the explicit Euler method for the pendulum problem. Both methods were trained with trajectories of length 20 and with the same amount of hyperparameters and training steps. The results are shown in Figure 1. This supports the assumption that the symplectic scheme trains more stable and with a smaller amount of hyperparameters than the standard approach.

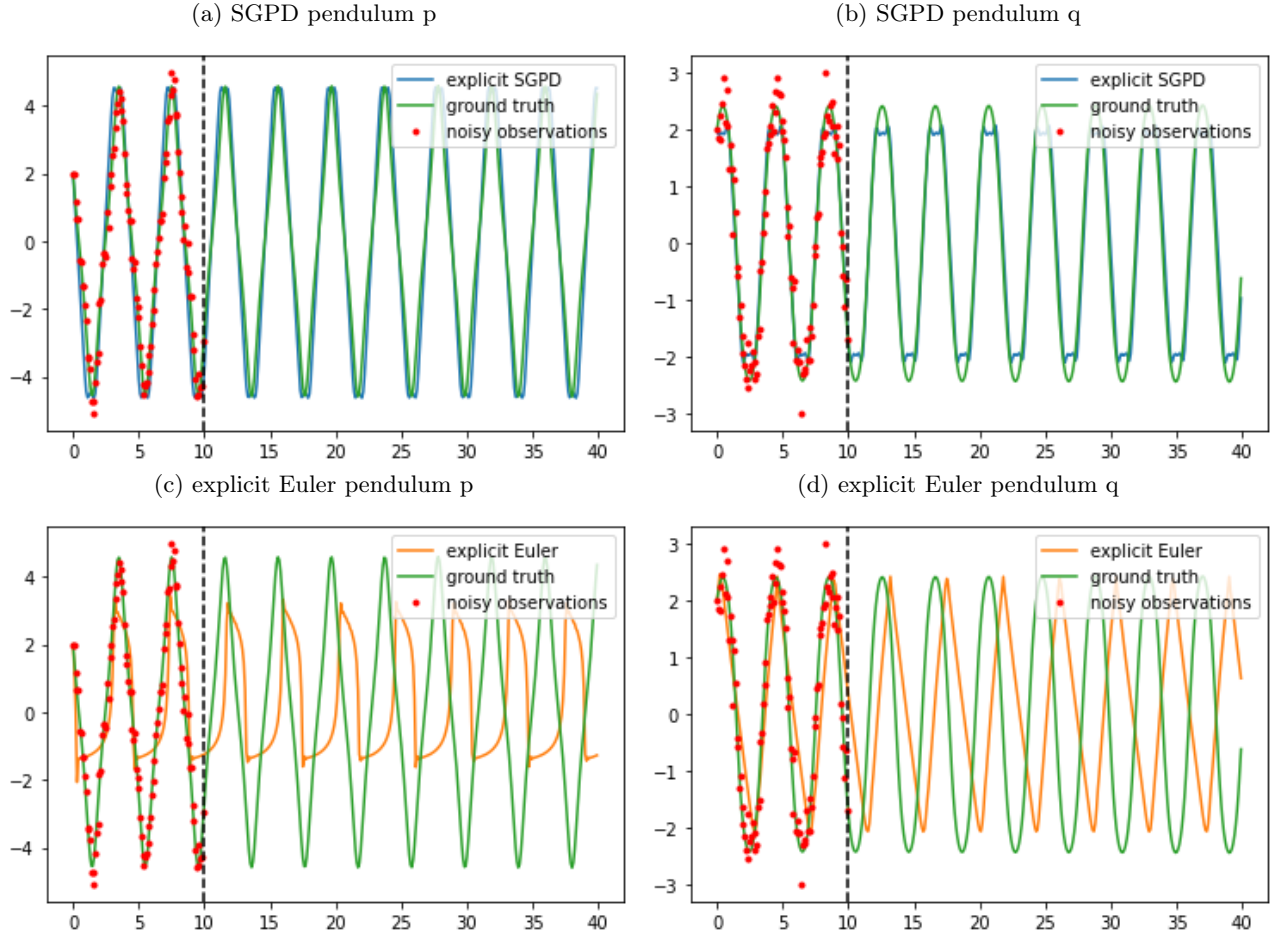


Figure 1: Results for longer training trajectories. Shown are rollouts over time for the SGPD 1a, 1b and the explicit Euler method 1c, 1d. The training horizon is marked with dotted lines.

3 Hyperparameters

Table 1 shows the initialization of the hyperparameters that were chosen for the experiments with separable Hamiltonians. Table 2 shows the initialization of the hyperparameters that were chosen for the experiments with non separable Hamiltonians. For each of the independent Gaussian processes f_i the same initialization was chosen. The total number of inducing inputs is denoted N_ξ .

Table 1: Hyperparameters separable Hamiltonian

method	σ_f^2	l_i^2	$\mu_{\xi,i}$	Σ_ξ	N_ξ	σ_n^2
explicit SGPD	0.1	$\sqrt{2}$	$\mathcal{N}(0, 0.05^2)$	$0.01 \cdot \mathbf{I}$	14	0.1
explicit Euler	0.01	$\sqrt{2}$	$\mathcal{N}(0, 0.05^2)$	$0.01 \cdot \mathbf{I}$	14	0.1

Table 2: Hyperparameters non separable Hamiltonian

method	σ_f^2	l_i^2	$\mu_{\xi,i}$	Σ_ξ	N_ξ	σ_n^2
implicit SGPD	0.1	2	$\mathcal{N}(0, 0.05^2)$	$0.0001 \cdot \mathbf{I}$	16	0.0005
explicit Euler	0.01	2	$\mathcal{N}(0, 0.05^2)$	$0.0005 \cdot \mathbf{I}$	16	0.0005

Bibliography

- Bijl, H., Schön, T., Wingerden, J. W., and Verhaegen, M. (2017). System identification through online sparse gaussian process regression with input noise. *IFAC Journal of Systems and Control*, 2:1–11.
- Deisenroth, M. P. and Rasmussen, C. E. (2011). Pilco: A model-based and data-efficient approach to policy search. In *In Proceedings of the International Conference on Machine Learning*.
- Rasmussen, C. E. and Williams, C. K. I. (2005). *Gaussian Processes for Machine Learning (Adaptive Computation and Machine Learning)*. The MIT Press.